Age-related dedifferentiation and hyperdifferentiation of perceptual and mnemonic representations

Lifu Deng[1,§], Simon W. Davis[1,2,§], Zachary A. Monge[1,§], Erik A. Wing[1,3], Benjamin R. Geib[1], Alex Raghunandan[1], and Roberto Cabeza[1*]

[1] Center for Cognitive Neuroscience, Duke University, Durham, NC 27708

[2] Department of Neurology, Duke University School of Medicine, Durham, NC 27710

[3] The Rotman Research Institute at Baycrest, Toronto, Ontario, Canada M6A 2E1

[§] These authors contributed equally to the study

[*]Address correspondence to:

Roberto Cabeza

Center for Cognitive Neuroscience, Duke University

Box 90999, Durham, NC 27708

Email: cabeza AT duke.edu

Abstract

Preliminary evidence indicates that occipito-temporal activation patterns for different visual stimuli are less distinct in older (OAs) than younger (YAs) adults, suggesting a dedifferentiation of visual representations with aging. Yet, it is unclear if this deficit (1) affects only sensory or also categorical aspects of visual representations, and (2) affects only perceptual or also mnemonic representations. To investigate these issues, we fMRI-scanned YAs and OAs viewing and then remembering visual scenes. First, using representational similarity analyses, we distinguished sensory vs. categorical features of

visual representations. We found that, compared to YAs, sensory features in early visual cortex were less differentiated in OAs (i.e., age-related dedifferentiation), replicating previous research, whereas categorical features in anterior temporal lobe (ATL) were more differentiated in OAs. This is, to our knowledge, the first report of an *age-related hyperdifferentiation*. Second, we assessed the quality of mnemonic representations by measuring encoding-retrieval similarity (ERS) in activation patterns. We found that aging attenuated ERS in early visual cortex and hippocampus but enhanced ERS in ATL. Thus, both visual and mnemonic representations in ATL were enhanced by aging. In sum, our findings suggest that aging impairs visual and mnemonic representations in posterior brain regions but enhances them in anterior regions.

Keywords: aging, perception, memory, functional MRI, representations.

1. Introduction

As we age, the anatomy and physiology of our brain declines, impairing cognitive abilities such as perception and memory (Grady, 2012; Grady, 2008). Most prior functional MRI (fMRI) studies investigating the neural bases of these impairments have focused primarily on *processes* (operations performed on information) and only rarely examined age effects on *representations* (the quality of information processed). However, there is fMRI evidence that activation patterns elicited by different types of visual stimuli (faces, places, etc.) are less distinct in older adults (OAs) than in younger adults (YAs; Chee et al., 2006; Goh et al., 2010; Park et al., 2004; Payer et al., 2006; Voss et al., 2008). This phenomenon, known as *age-related neural dedifferentiation*, suggests that aging impairs the quality of visual representations. Yet, two fundamental questions remain unanswered: (1) what aspects of visual representations are impaired by aging? and (2) do age-related deficits in visual representations impair downstream representations such as visual memory traces? The current study investigates these two critical questions.

1. *What aspects of the visual representations are impaired by aging?* This is a critical issue because visual representations consist of multiple features, which are processed in different brain regions and are affected differentially by aging. In particular, it is well established that sensory features are processed primarily in early visual cortex and that these sensory features form conjunctions of categorical features in more anterior ventral pathway regions, such as the anterior temporal lobe (ATL; Bussey et al., 2005; Clarke and Tyler, 2014). The sensory-to-categorical feature distinction is relevant to aging because OAs tend to be impaired in processes utilizing sensory features (e.g., sensory processing) but not in processes more reliant on categorical features (e.g., conceptual and semantic processing; Cherry et al., 2012; Mohanty et al., 2016; Monge and Madden, 2016; Owsley, 2011). Thus, we hypothesized that *age-related visual dedifferentiation impairs sensory features in early visual cortex but not categorical features in the ATL* (**Hypothesis 1**). Given than some aspects of categorical-related

processing are actually better in OAs than YAs (Long and Shaw, 2000; Park et al., 2002), an intriguing possibility is that categorical features in the ATL could be enhanced by aging.

We investigated Hypothesis 1 using representational similarity analyses (Kriegeskorte and Kievit, 2013; Kriegeskorte et al., 2008), in which similarity across stimuli are coded by different *stimuli models*. In the *sensory model*, stimuli similarity is based on sensory visual features, such as shape (e.g., gun ≈ hair dryer), whereas in the *categorical model*, it is based on categorical features (e.g., gun ≈ sword). The stimuli model is then correlated with similarity in fMRI activation patterns for the same set of stimuli. The resulting *model-brain fit* (2^{nd} order correlation) identifies brain regions that process and/or store representations emphasizing sensory and/or categorical visual features (**Fig. 1a**). As stimuli models code the differences between images based upon a feature of interest (e.g., sensory, categorical), model-brain fit may be interpreted as a measure of differentiation, where higher values in a brain region indicate greater neural differentiation.

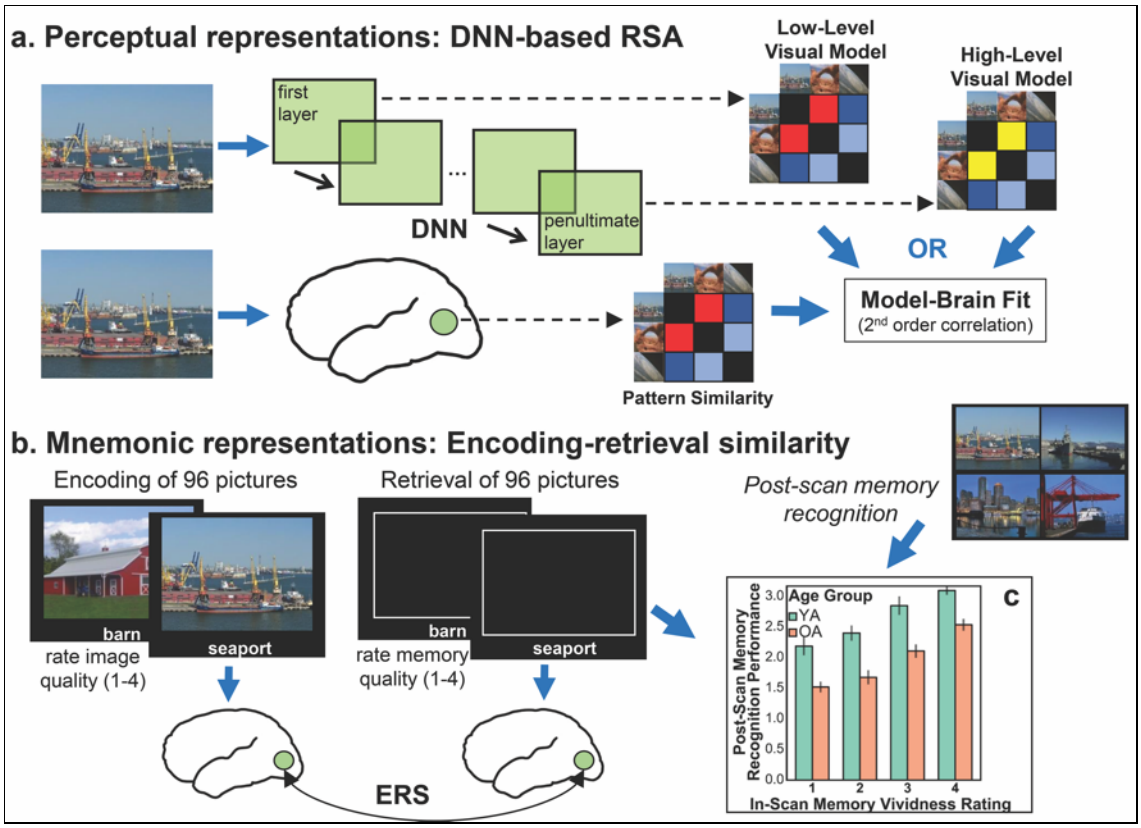

Figure 1: *Perceptual and mnemonic representations analysis approach.*

Panel a *shows a model of the analysis combining representational similarity analysis and DNN layers. To create models from DNN layers, the image stimuli are submitted to the pre-trained DNN and at each layer of interest, the "activation" values are extracted. Here, our layers of interest were the first and penultimate layers. For each image and layer of interest, the vectors of activation values are correlated with each other resulting in a stimuli model for each layer of interest. The stimuli models may then be used to predict brain activation patterns (model-brain fit).* ***Panel b*** *shows our paradigm in which participants, while undergoing fMRI scanning, studied images (while rating the quality of the images) and later retrieved their memories of the scenes (while rating the vividness of their memories). We quantified the similarity of encoding to retrieval representations by calculating ERS.* ***Panel c*** *shows for each in-scan vividness rating value, the corresponding post-scan memory recognition performance; the corresponding post-scan memory recognition performance reflects the average score (0=Miss, 1=Hit [confidence 1], 2=Hit [confidence 2], 3=Hit [confidence 3], 4=Hit [confidence 4]). The in-scan vividness ratings were related to post-scan memory recognition performance; error bars represent the standard error of the mean. ERS = encoding-retrieval similarity; DNN = deep convolutional neural network; fMRI = functional MRI; OA = older adult; RSA = representational similarity analysis; YA = younger adult.*

In the current study, our stimuli models were derived from *deep convolutional neural networks* (DNNs; Krizhevsky et al., 2012; LeCun et al., 2015). DNNs consist of layers of convolutional filters and can be trained to classify images into categories with a high level of accuracy. During training, DNNs "learn" convolutional filters in service of classification, where filters from early layers predominately detect sensory features and from late layers, categorical features (Zeiler and Fergus, 2014). Previous work has demonstrated that DNNs model representations along the ventral visual pathway, where early layers map brain activation patterns predominately in early visual cortex and late layers map brain activation patterns in more anterior ventral visual pathway regions (Güçlü and van Gerven, 2015; Khaligh-Razavi and Kriegeskorte, 2014; Kriegeskorte, 2015; Leeds et al., 2013; Wen et al., 2017). With models traditionally used to map brain activation patterns it is difficult to model this hierarchy of sensory to categorical features, especially with scenes where their categories are less clear. DNNs allow for this hierarchy to be investigated within a single framework. Furthermore, DNNs outperform traditional theoretical models of the ventral visual pathway (e.g., HMAX, object-based models; Cadieu et al., 2014; Groen et al., 2018). Therefore, a DNN is an ideal model to investigate this sensory-to-categorical

feature distinction. Here, we used a pre-trained 16-layer DNN, the VGG16 (Simonyan and Zisserman, 2014), which was successfully trained to classify 1.8 million scenes into 365 categories (Zhou et al., 2017). The first layer generated a *sensory model*, since this model is derived from a layer that detects sensory features, and the penultimate layer, a *categorical model*, since this model is derived from the layer before the images are explicitly categorized into the trained categories (Bankson et al., 2018; Devereux et al., 2018; Groen et al., 2018).

Given the posterior-anterior organization of the ventral visual pathway, we expected that the sensory model would correlate with activation patterns in early visual cortex, and the categorical model, with activation patterns in ATL. On the basis of Hypothesis 1, we predicted that, compared to YAs, (1) the correlation between brain activation patterns and the sensory model (i.e., model-brain fit) would be reduced in OAs, whereas (2) the correlation between brain activation patterns and the categorical model would be spared (or even enhanced) in OAs.

2. *Do age-related deficits in visual representations impair downstream representations such as visual memory traces?* Age-related sensory and cognitive deficits are strongly related to each other (Baltes and Lindenberger, 1997; Lindenberger and Baltes, 1994), possibly because sensory deficits cascade through the cognitive system impairing downstream cognitive processes (Monge and Madden, 2016). Consistent with this idea, degrading stimuli (i.e., mimicking sensory impairment) by adding noise yields cognitive deficits in YAs that resemble cognitive deficits in OAs (Gilmore et al., 2006; Monge and Madden, 2016; Murphy et al., 2000; Pichora-Fuller et al., 1995). In contrast, spared categorical processing in OAs may explain why age-related memory deficits are attenuated for semantically-rich stimuli (Kausler, 1994; Naveh-Benjamin, 2000). Thus, the sensory to categorical dissociation we postulated for perceptual representations (Hypothesis 1) is likely to apply also to mnemonic representations. In the case of mnemonic representations, however, the age-related deficit is likely to affect not only visual cortex but also downstream memory-binding regions, such as the hippocampus. Thus, we hypothesized that *aging impairs mnemonic representations for sensory features in the early*

visual cortex and hippocampus but preserved, or possibly even enhanced, categorical features in the ATL (**Hypothesis 2**).

We investigated Hypothesis 2 using a reactivation fMRI paradigm (Danker and Anderson, 2010; Rugg and Vilberg, 2013). As illustrated by **Fig. 1b**, during encoding scans, samples of YAs and OAs viewed 96 pictures of scenes paired with labels, and during retrieval scans, they recalled the scenes in response to the labels and rated the quality of their memories. These in-scan ratings were validated with a post-scan forced-choice memory recognition test, which showed that greater in-scan ratings were associated with better post-scan accuracy (**Fig. 1c**; see the Materials and Methods for more details on participants and the experimental design). Previous reactivation fMRI studies with OAs compared broad categories of stimuli (Abdulrahman et al., 2017; Johnson et al., 2015; Thakral et al., 2019; Wang et al., 2016) or presented stimuli multiple times during encoding (St-Laurent et al., 2014), precluding reactivation measures for individual events. In contrast, we measured the reactivation of individual events (each scene) by directly measuring *encoding-retrieval similarity* (ERS) in activation patterns (Ritchey et al., 2013; Wing et al., 2014). On the bases of Hypothesis 2, we predicted that, compared to YAs, OAs would show reduced ERS in the early visual cortex but spared (or even enhanced) ERS in the ATL.

2. Materials and Methods

2.1. Study Participants

Our study sample included 22 YAs and 22 OAs. One YA and one OA were excluded from analysis because of functional data missing from the first fMRI run due to a technical error. Another OA was excluded from analysis due to a poor quality T1 image, not allowing the participant's functional images to be properly normalized into MNI space. This left a study sample of 21 YAs (12 women, age range = 18-30 years, *M* = 23.5 years, *SD* = 3.0 years) and 20 OAs (9 women, age range = 61-82 years, *M* = 70.5 years, *SD* = 5.4 years). Participants self-reported to be free of significant health

problems (including atherosclerosis, neurological and psychiatric disorders), and not taking medications known to affect cognitive function or cerebral blood flow (except antihypertensive agents). Also, all participants were right-handed and completed at least 12 years of education. The OAs were additionally screened for dementia via the Mini-Mental State Examination (MMSE; inclusion criterion ≥ 27; M = 29.2, SD = 0.7; Folstein et al., 1975); no exclusions were necessary based upon this criterion. After study completion, participants were monetarily compensated for their time. Study results from the sample of YAs were previously reported in other manuscripts (Geib et al., 2017; Wing et al., 2014). The Duke University Institutional Review Board approved all experimental procedures, and participants provided informed consent prior to testing.

2.2. Experimental Design

Participants completed three encoding runs followed by three retrieval runs. During the encoding runs, participants explicitly studied a total of 96 pictures of complex scenes (32 images per run, order randomized within run). During each encoding trial (4 sec), participants were presented a single picture with a short descriptive label below the image (e.g., “tunnel” or “barn”). Within the trials, participants were asked to rate, on a four-point scale (1 = *low quality*, 4 = *high quality*), the quality of the image. This was to ensure participants would pay attention to the details of each image. Each encoding trial was followed by an active baseline interval of 8 sec, in which participants were presented digits from 1 to 4 and pushed the button corresponding to the presented numbers.

The retrieval runs were identical in format to the encoding runs, except the pictures of the scenes were not presented. During each retrieval trial, participants were presented the descriptive scene label previously presented with the picture of the scene, and participants were instructed to recall the corresponding image from encoding with as much detail as possible. Participants then rated, on a four-point scale, the amount of detail with which they could remember for the specific picture (1 = *least amount of detail*, 4 = *highly detailed memory*).

2.3. MRI Data Acquisition

MRI data were collected on a General Electric 3T MR750 whole-body 60 cm bore MRI scanner and an 8-channel head coil. The MRI session started with a localizer scan, in which 3-plane (straight axial/coronal/sagittal) localizer faster spin echo (FSE) images were collected. Following, using a SENSE spiral-in sequence (repetition time [TR] = 2000 msec, echo time = 30 msec, field of view [FOV] = 24 cm, 34 oblique slices with voxel dimensions of 3.75 x 3.75 x 3.8 mm^3), the functional images were acquired. The functional images were collected over six runs – three encoding runs and three retrieval runs; there was also a functional resting-state run after the third encoding run, which is not reported here. Stimuli were projected onto a mirror at the back of the scanner bore, and responses were recorded using a four-button fiber-optic response box (Current Designs, Philadelphia, PA, USA). Following, a high-resolution anatomical image (96 axial slices parallel to the AC-PC plane with voxel dimensions of 0.9 x 0.9 x 1.9 mm) was collected. Finally, diffusion-weighted images were collected, which are not reported here. Participants wore earplugs to reduce scanner noise, and foam pads were used to reduce head motion, and, when necessary, participants wore MRI-compatible lenses to correct vision.

2.4. Functional MRI Data Preprocessing

For each run, the first six functional images were discarded to allow for scanner equilibrium. All functional images were preprocessed in a SPM12 (London, United Kingdom; http://www.fil.ion.ucl.ac.uk/spm/) pipeline. Briefly, the functional images were slice timing corrected (reference slice = first slice), realigned to the first scan in the first session, and subsequently unwarped. Following, the functional images were coregistered to the skull-stripped high-resolution anatomical image (skull-stripped by segmenting the high-resolution anatomical image and only including the gray matter, white matter, and cerebrospinal fluid segments). The functional images were normalized into MNI space using DARTEL (Ashburner, 2007); the study specific high-resolution anatomical image was created using all of the study participants. The voxel size was maintained at 3.75 x 3.75 x 3.8 mm^3 and

the normalized-functional images were not spatially smoothed. Lastly, the DRIFTER toolbox (Sarkka et al., 2012) was used to denoise the functional images.

2.5. Functional MRI Analysis

2.5.1. Functional Representational Similarity

To obtain the beta estimates for each event, we conducted a single-trial model analysis within a general linear model. These beta estimates were calculated using a least squares-separate approach (Mumford et al., 2012). This approach estimates a first-level model in which one regressor models a specific event of interest and another regressor models all the other events (each run included a regressor modeling these other trials). Each event was modeled with a stick function placed at stimulus onset convolved with a standard hemodynamic response function with the temporal and dispersion derivative. Each model also included the six raw motion regressions, a composite motion parameter (derived from the Artifact Detection Tools [ART]), outlier TRs (scan-to-scan motion > 2.0 mm or degrees, scan-to-scan global signal change > 9.0 *z* score; derived from ART), the white matter timeseries, and cerebrospinal fluid timeseries. In each model we also modeled the temporal and dispersion derivatives and implemented a 128 sec cutoff high-pass temporal filter. These beta-images were used for (1) the representational similarity analysis combined with DNNs and (2) ERS. These analyses were conducted using in-house MATLAB (Natick, MA, USA) scripts (https://github.com/brg015). For the ERS analyses, we excluded trials in which participants responded (during retrieval) either not at all or in less than 250 msec.

2.5.2. Representational Similarity Analysis Combined with Deep Convolutional Neural Networks

To examine our first goal, we combined representational similarity analysis (Kriegeskorte and Kievit, 2013; Kriegeskorte et al., 2008) and stimuli models derived from DNNs (Khaligh-Razavi and Kriegeskorte, 2014; Kriegeskorte, 2015; Leeds et al., 2013; Wen et al., 2017). The stimuli models (96 x

96 matrix) from each layer of interest were correlated (Spearman correlation) with the brain activation patterns similarity matrix (96 x 96 matrix) derived from searchlight spheres. For the searchlight analysis (Kriegeskorte et al., 2006), a 5 x 5 x 5 voxel cube (Wing et al., 2014) was placed around a voxel location and the activation values from this cube were extracted and vectorized. At the voxel location, this procedure was conducted for each stimulus and the activation values from each stimulus were correlated (Fisher-transformed Pearson's *r*) with each other, representing the brain activation patterns. The brain activation patterns were then correlated (Spearman's correlation) with the DNN-stimuli models (model-brain fit), which was the value placed in the voxel location. This procedure was repeated for every voxel in the brain and the output of this analysis was searchlight volumes representing brain activation pattern-DNN layer stimuli model similarity.

For the DNN, we used the popular VGG16 (Simonyan and Zisserman, 2014) pre-trained on approximately 1.8 million images of scenes in service of categorizing the images into 365 scene categories (Zhou et al., 2017). The VGG16 consists of 13 convolutional layers and 3 fully-connected layers. We created stimuli models from the first DNN layer (reflecting sensory features) and penultimate DNN layer (reflecting categorical features). It should be noted that we chose these two layers because they reflect the extremes of the DNN, but that stimuli models constructed from surrounding layers are correlated with each other (Supplementary Fig. 1). These stimuli models were constructed by feeding the study stimuli through the pretrained DNN and for each stimulus at each layer of interest (i.e., the first and penultimate layers), extracting the activation values. For each layer of interest, the activation values between stimuli were correlated (Pearson correlation) with each other. This yielded two 96x96 matrices (one for each layer of interest), which represent the similarity of the DNN activation values and are the image models (sensory and categorical image models).

After conducting the searchlight analysis examining model-brain fit, the searchlight volumes were spatially smoothed with a 5 mm Gaussian kernel (Clarke et al., 2016; Clarke and Tyler, 2014). Then, for each model, we extracted model-brain fit from *a priori* ROIs derived from the AAL atlas (Tzourio-Mazoyer et al., 2002), which consisted of early visual cortex (bilateral calcarine, cuneus, and

lingual ROIs) and ATL (left dorsal temporal pole and ventral temporal pole). We chose to examine only the left ATL because of our interest in categorical representations and an extensive literature demonstrating greater processing of categorical-related features (e.g., conceptual processing) in the left hemisphere (Hodges et al., 1992; Tyler et al., 2004; Warrington and McCarthy, 1983). See the Introduction for an explanation of *a priori* ROI choice.

2.5.3. Encoding-Retrieval Similarity

To examine our second goal, we calculated ERS for each item using a searchlight procedure (Kriegeskorte et al., 2006). For each item, encoding and retrieval activation values were extracted from searchlight spheres and the encoding and retrieval vectors were correlated with each other. A 5 x 5 x 5 voxel cube was placed around each voxel and the activation values were extracted and vectorized. For each item, the encoding and retrieval vectors were correlated and the resulting correlation value (Fisher-transformed Pearson's *r*, which is ERS) was placed in the original voxel location. Within each voxel location, the ERS value for each stimulus (a total of 96 values for each image) was averaged across all stimuli. This procedure was repeated for every voxel within the brain. Afterwards, the searchlight volumes were spatially smoothed with a 5 mm Gaussian kernel (Clarke et al., 2016; Clarke and Tyler, 2014). We then extracted ERS from *a priori* ROIs derived from the AAL atlas (Tzourio-Mazoyer et al., 2002), which consisted of early visual cortex (bilateral calcarine, cuneus, and lingual ROIs), ATL (left dorsal temporal pole and ventral temporal pole), and the hippocampus (bilateral hippocampi). See the Introduction for an explanation of *a priori* ROI choice. In addition to item-level ERS, as a control analysis, we also calculated set-level ERS, which is ERS between an item and every other item within the set (Ritchey et al., 2013; Wing et al., 2014); this analysis was constrained to the items that were subsequently remembered on the post-scan memory task.

2.6. VGG16 Fine-Tuning

In our preliminary analysis validating the VGG16 as a model of low- to categorical representations in our study (see Results), we fine-tuned the VGG16 to classify our images into indoor

vs. outdoor pictures. This was achieved by removing the last layer of the VGG16 and adding a layer with two outputs (with a softmax activation function), corresponding to indoor and outdoor scenes. The revised VGG16 was then trained using three pictures from each image category (images from the post-scan recognition task besides the target images) and tested on the pictures presented within the scanner. After 30 epochs, the revised VGG16 was able to classify the images (indoor vs. outdoor) with 94.8% accuracy. The revised VGG16 was only used for this preliminary analysis.

2.7. Statistical Analysis

All statistical analyses (unless otherwise stated) were conducted within StatsModels (Seabold and Perktold, 2010) ran in Python 3 (Python Software Foundation, https://www.python.org/) using two-sided linear mixed effects models. Before entering the data into the linear mixed effects models, all values were *z*-transformed. For the analyses statistically controlling for SNR, SNR was entered into the model as a nuisance variable. All effect sizes reported in the manuscript were Cohen's *d*.

3. Results

3.1. Preliminary analyses

Before testing our two hypotheses, we conducted two preliminary analyses to validate the VGG16 (Simonyan and Zisserman, 2014) as a model of sensory to categorical representations in our study. First, the VGG16 was already successfully trained to classify 1.8 million scenes into 365 categories (Zhou et al., 2017), but we wanted to confirm it could also classify the 96 images employed in our study. Given that some of the scene labels we used (e.g., seaport, Fig. 1-B) are different than the categories used to train the VGG16, we used instead a binary indoor-outdoor scene classification (see the Materials and Methods for more details). The VGG16 achieved this classification with 94.8% accuracy. It should be noted that the model with this binary indoor-outdoor scene classification was only used to validate the use of the VGG16 within our study; the pretrained VGG16 was used for stimuli

model construction. Second, we correlated the sensory and categorical stimuli models and found that they were only moderately correlated with each other (r = 0.32), indicating that each model represents unique features. Having confirmed the validity of VGG16, we turned to our two hypotheses.

3.2. Perceptual representations: DNN-based representational similarity analysis

Our first hypothesis was that age-related visual dedifferentiation impairs the differentiation of sensory features in early visual cortex but not categorical features in the ATL, which may even be enhanced in aging. Using DNN-based representational similarity analysis, we tested this hypothesis by comparing age-related differences in model-brain fit for the sensory model based on the first VGG16 layer and for the categorical model based on the penultimate VGG16 layer. We tested this hypothesis in two *a priori* ROIs – early visual cortex and ATL. As illustrated in **Fig. 2a**, which shows z-scored 2nd order correlations, the evidence was consistent with our first hypothesis: compared to the YAs, in early visual cortex, the sensory model-brain fit was reduced in the OAs (β = -0.39, z = 19.86, p < .0001, d = 0.83), whereas in the ATL (β = 0.26, z = 12.82, p < .0001, d = 0.53), the categorical model-brain fit was enhanced in the OAs (see Supplementary Fig. 2a for raw model-brain fit values). In other words, whereas early visual cortex showed age-related *de*differentiation, the ATL showed age-related *hyper*differentiation. As the ATL is particularly vulnerable to low signal-to-noise ratio (SNR), we repeated the analysis statistically controlling for SNR and still found that in the ATL that categorical model-brain fit was enhanced in the OAs compared to YAs (β = 0.26, z = 15.61, p < .0001). We did not find statistically significant age-group differences of the sensory model-brain fit in the ATL (β = 0.17, z = 1.39, p = .17, d = 0.33), but we did find, compared to YAs, that the categorical model-brain fit in the early visual cortex was reduced in the OAs (β = -0.27, z = 3.25, p < .01, d = 0.54). In sum, this is, to our knowledge, the first evidence of age-related hyperdifferentiation of activation patterns in the ventral pathway or any brain region.

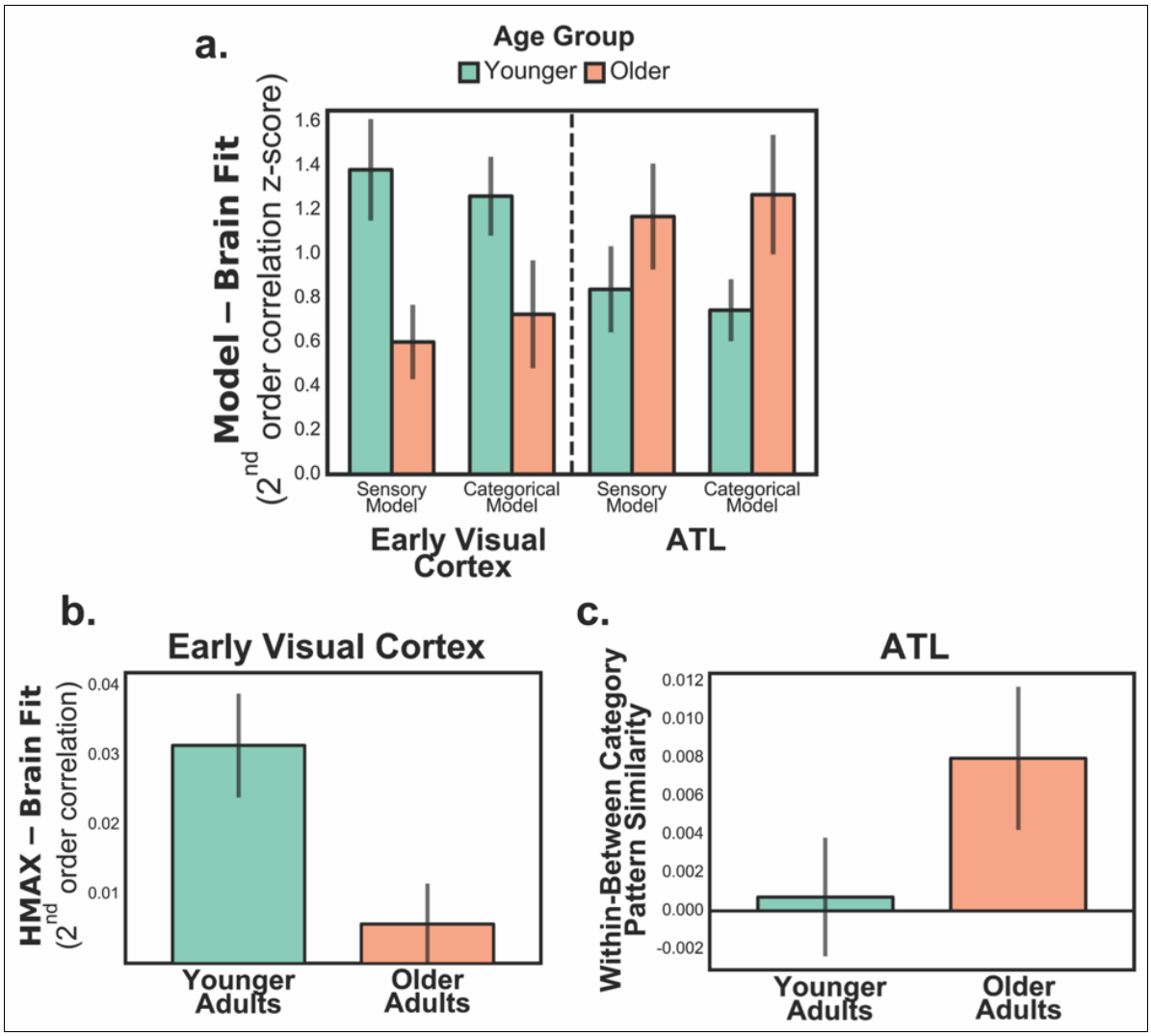

Figure 2: *Age-related neural dedifferentiation and hyperdifferentiation.*

Panel a *shows within the early visual cortex and ATL the stimuli model (sensory and categorical)-brain fit; the figure shows z-scored (mean set to one) 2nd order correlations. Compared to the YAs, in the early visual cortex, we found that the sensory model-brain fit was reduced in the OAs (age-related dedifferentiation), whereas in the ATL, the categorical model-brain fit was enhanced in the OAs (age-related hyperdifferentiation).* ***Panel b*** *shows the HMAX C1 response model-brain fit in early visual cortex. We found that, compared to YAs, OAs exhibited reduced HMAX-brain fit in early visual cortex.* ***Panel c*** *shows the brain activation pattern similarity for within-categories – between-categories (categories = indoor vs. outdoor scenes) in the ATL. We found that, compared to the YAs, OAs exhibited enhanced activation pattern similarity for within- than between-categories in the ATL. Error bars represent the standard error of the mean. Error bars represent the standard error of the mean. ATL = anterior temporal lobe, OAs = older adults, YAs = younger adults.*

Although the *a priori* ROI analysis was used to test our hypothesis, as an exploratory analysis, we conducted the whole-brain searchlight analysis. Consistent with previous research that early DNN layers identified posterior brain regions mediating sensory representations, and later layers, anterior brain regions mediating categorical representations (Güçlü and van Gerven, 2015; Khaligh-Razavi and Kriegeskorte, 2014; Kriegeskorte, 2015; Leeds et al., 2013; Wen et al., 2017), within both the OAs and YAs, the first layer of the VGG16 was primarily associated with visual cortices and the penultimate layer was additionally linked to anterior temporal, parietal, and frontal regions (shown in unthresholded, color-coded maps in **Fig. 3**; see Supplementary Table 1 for cluster coordinates). Qualitatively, in these maps, it can be seen that the sensory model is more strongly associated with earlier visual cortex region activation patterns in YAs than OAs, whereas the categorical model is more strongly associated with more anterior ventral visual pathway region, such as the ATL, activation patterns in OAs than YAs (see white arrows). In sum, the whole-brain searchlight analysis largely mirrors the *a priori* ROI analysis.

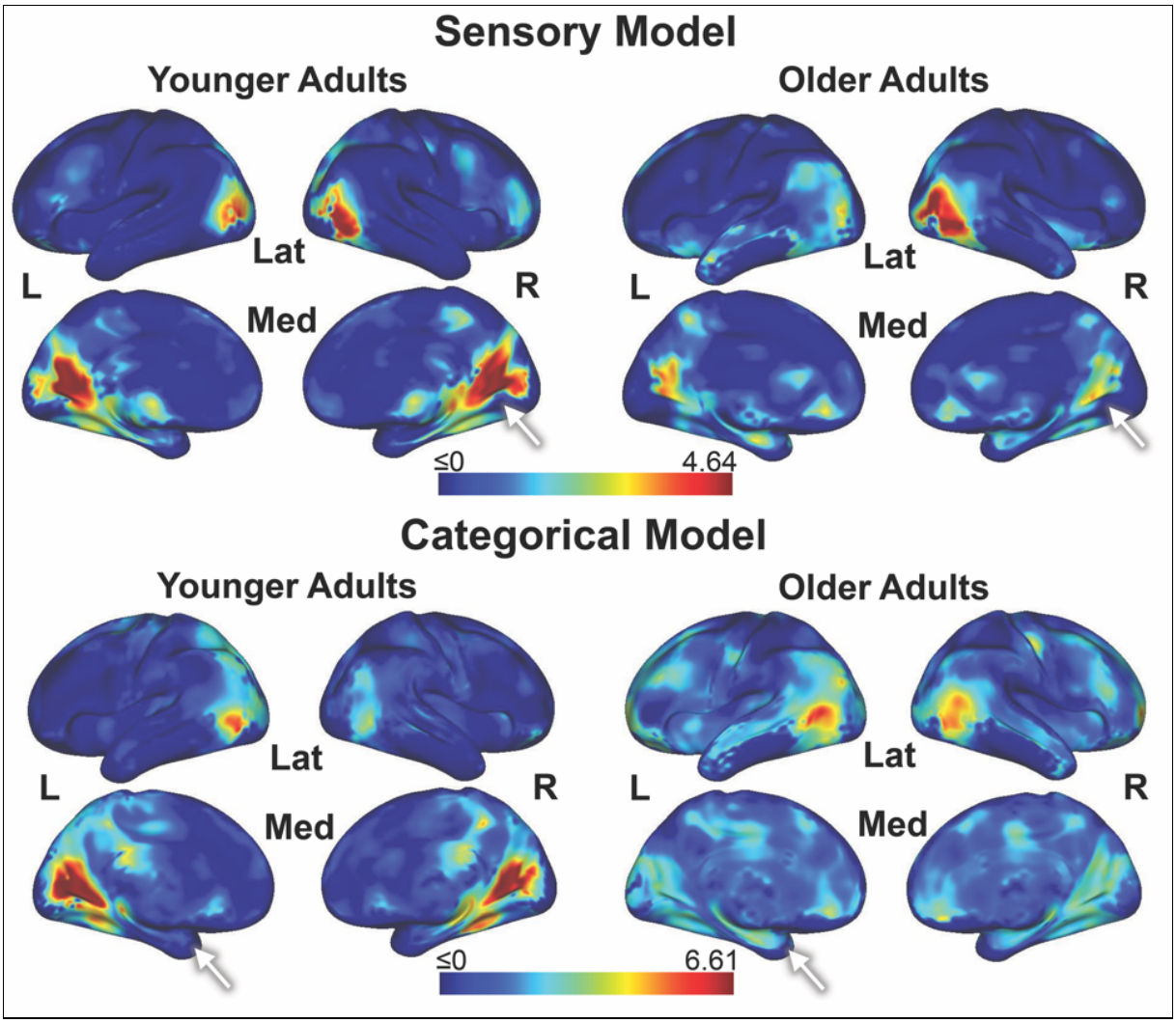

Figure 3: *Sensory and categorical model-brain fit.*

The figure shows the whole-brain searchlight analysis of the stimuli model (sensory and categorical)-brain fit. Within both the YAs and OAs, we found that the sensory model (based upon the first DNN layer) correlated predominately with brain activation patterns in the visual cortices and the categorical model (based upon the penultimate DNN layer) additionally correlated with brain activation patterns in anterior temporal, parietal, and frontal regions. Qualitatively, in these maps it can be seen that that the sensory model is more strongly associated with earlier visual cortex region activation patterns in YAs than OAs, whereas the categorical model is more strongly associated with more anterior ventral visual pathway region, such as the ATL, activation patterns in OAs than YAs (see white arrows). DNN = deep convolutional neural network; L = left; Lat = lateral; Med = medial; OAs = older adults; R = right; YAs = younger adults.

Although DNNs provide stronger models of visual representations in the ventral visual pathway than traditional theoretical models (e.g., HMAX, object-based models; Cadieu et al., 2014; Groen et al., 2018) and we believe are an ideal model to investigate this sensory to categorical feature distinction, DNNs are sometimes critiqued for being too complex and, therefore, less interpretable. We believe that this level of complexity is necessary to map representations within the brain and that DNNs are one of the few models available that are complex enough to map fMRI representations (Kriegeskorte and Douglas, 2018), but the critique of interpretability is well received. Therefore, we examined age-related differences in the *a priori* ROIs using more traditional models. For sensory representations, we used the C1 responses of the HMAX model (Clarke and Tyler, 2014; Serre et al., 2007), which are proposed to reflect properties of early visual cortex (Riesenhuber and Poggio, 1999; Serre et al., 2007), and for categorical representations, we examined brain activation pattern similarity for within- compared to between-categories (indoor vs. outdoor scene trials). For the categories, we chose indoor and outdoor scenes because these categories likely share large amounts of objects and visual features, as demonstrated in our preliminary analysis using the VGG16 to classify indoor and outdoor scenes (see Preliminary analyses in the Results). Consistent with the DNN analysis, compared to the YAs, the OAs exhibited reduced model-brain fit with the HMAX model in early visual cortex (**Fig. 2b**; β = -0.39, z = 13.73, p < .0001, d = 0.82), but enhanced activation pattern similarity for within- than between-categories in the ATL (**Fig. 2c**; β = 0.23, z = 3.36, p < .001, d = 0.46; see Supplementary Fig. 2b for pattern similarity values of each category). These findings provide further evidence for age-related dedifferentiation of sensory features in early visual cortex and hyperdifferentiation of categorical features in ATL.

3.3. Mnemonic representations: Encoding-retrieval similarity

Our second hypothesis was that aging impairs mnemonic representations for sensory features in early visual cortex and hippocampus but not for categorical features in the ATL. To test this hypothesis, we calculated encoding-retrieval similarity (ERS; Ritchey et al., 2013; Wing et al., 2014). We tested this

hypothesis using the same *a priori* ROIs used to test our first hypothesis with the addition of the hippocampus because of the second hypothesis's relation to memory (see the Methods for more details). Consistent with Hypothesis 2, as shown within **Fig. 4a**, we found that, compared to YAs, OAs exhibited reduced ERS in the early visual cortex (β = -0.35, z = 14.34, p < .0001, d = 0.74) and hippocampus (β = -0.45, z = 3.37, p < .001, d = 0.97), but increased ERS in the ATL (β = 0.20, z = 3.62, p < .001, d = 0.39; see Supplementary Fig. 2c for raw ERS values). As the ATL is particularly vulnerable to low SNR, we repeated the analysis statistically controlling for SNR and still found the same effect within the ATL (β = 0.24, z = 2.98, p < .01). In sum, it appears that aging impairs mnemonic representations within regions associated with sensory features but enhances mnemonic representations within regions associated with categorical features.

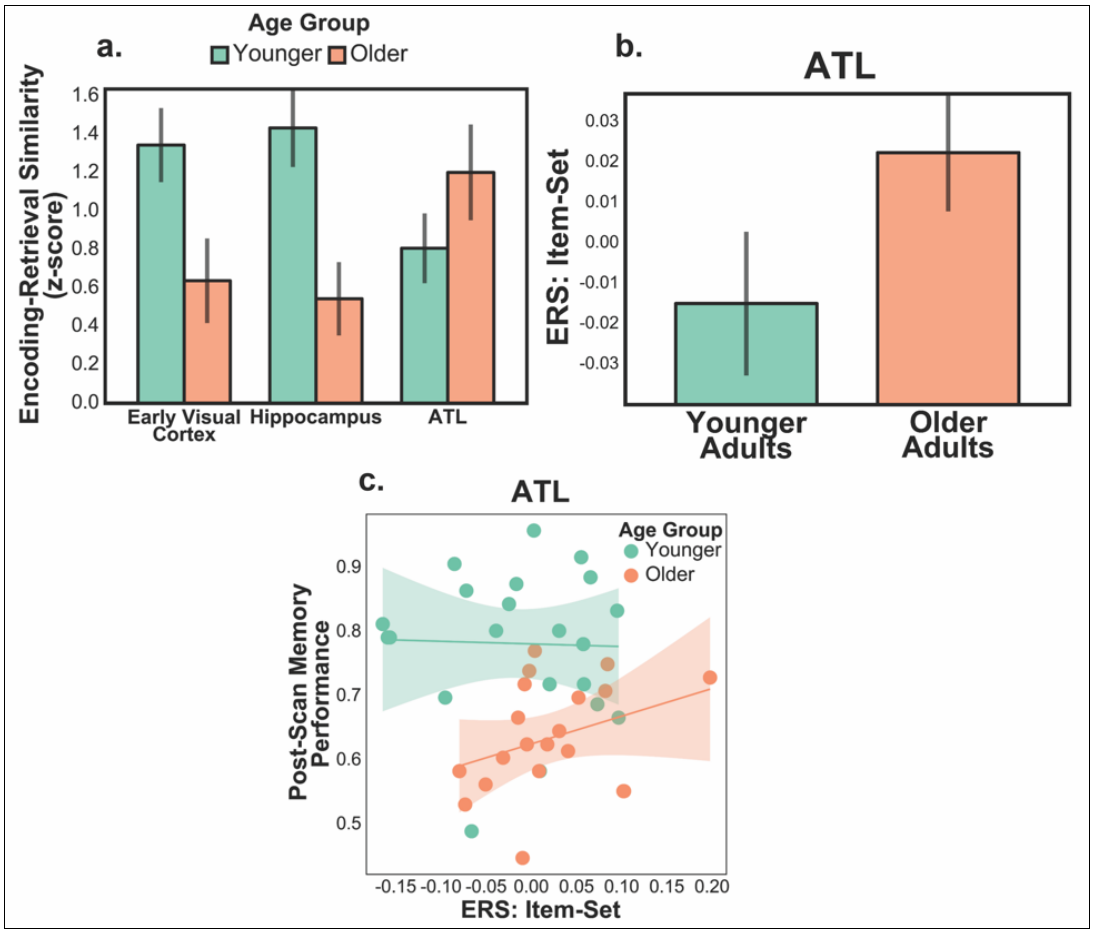

Figure 4: *Age-related differences in mnemonic representations.*

Panel a *shows age-related differences in ERS. We found, compared to the YAs, in the early visual cortex and hippocampus that the OAs exhibited reduced ERS, whereas in the ATL, the OAs exhibited increased ERS. The figure shows z-scored (mean set to one) ERS; error bars represent the standard error of the mean.* ***Panel b*** *shows item-specific ERS (item-set level ERS) in the ATL for trials that were subsequently remembered on the post-scan memory recognition task. We found that, compared to the YAs, OAs exhibited enhanced item-specific ERS in the ATL. Error bars represent the standard error of the mean.* ***Panel c*** *shows the relation between item-specific ERS in the ATL (limited to the trials that were subsequently remembered) and performance on the post-scan memory recognition task. We found in the OAs that increased item-specific ERS in the ATL was associated with better performance on the post-scan memory recognition task; translucent bars around the regression lines represent the 95% confidence intervals. ATL = anterior temporal lobe; ERS = encoding-retrieval similarity; OAs = older adults; YAs = younger adults.*

Within the previous analysis we examined ERS for individual items (i.e., item-level ERS). However, in order to make the claim that ERS is item-specific, it is necessary to also compare item-level ERS with set-level ERS (i.e., ERS between an item and the rest of the set; Koen and Rugg, 2016; Ritchey et al., 2013; Wing et al., 2014). Furthermore, in order to strengthen our claim that ERS here reflects memory, it is necessary to repeat the analysis only on items that were subsequently remembered on the post-scan memory recognition task. Therefore, we repeated the analysis subtracting set-level ERS from item-level ERS and only including trials that were subsequently remembered on the post-scan memory task. The only region that still exhibited the same age group difference pattern was the ATL, in which, compared to YAs, OAs exhibited enhanced ERS in the ATL (**Fig. 4b**; β = 0.25, z = 2.99, p < .01, d = 0.49; see Supplementary Fig. 2d for raw ERS values). The age-related increase in item-specific ERS in the ATL suggests that this region contributes to memory to a greater extent in OAs than YAs. To investigate this idea, we examined the relation between item-specific ERS (item-set ERS) in the ATL and performance on the post-scan memory recognition task. As illustrated in **Fig. 4c**, greater ATL item-specific ERS was associated with better performance on the post-scan memory recognition task in the OAs (β = 0.34, z = 4.07, p < .0001) but not YAs (β = -0.03, z = 0.48, p = .64); it should be noted,

however, that the age group by ERS interaction was not statistically significant (β = 0.15, z = 1.07, p = .28).

In sum, consistent with our second hypothesis, we found that OAs exhibited reduced ERS in the visual cortex and hippocampus but increased ERS in the ATL. The latter effect was found to be item specific and related to better memory performance in the OAs, suggesting that ATL hyperdifferentiation enhances the contributions of ATL to memory in OAs.

4. Discussion

The overarching goal of the study was to examine age-related differences in the quality of perceptual and mnemonic representations. We had two main findings. First, in early visual cortex, activation patterns associated with sensory features showed dedifferentiation in OAs, replicating previous age-related dedifferentiation findings, whereas in the ATL, activation patterns associated with categorical features showed hyperdifferentiation in OAs. This is, to our knowledge, the first report of age-related hyperdifferentiation. Second, for mnemonic representations, we found that increased age was associated with attenuated ERS (i.e., memory reactivation) in the early visual cortex and hippocampus but enhanced ERS in the ATL. The enhanced ERS in the ATL was associated with better memory in OAs, suggesting a compensatory mechanism. These findings are discussed in greater detail below.

4.1. Age-related neural dedifferentiation and hyperdifferentiation

Several studies have previously found evidence for age-related neural dedifferentiation (Carp et al., 2011; Chee et al., 2006; Goh et al., 2010; Payer et al., 2006; Voss et al., 2008) but these studies did not examine the specific aspects of visual representations that are impaired by aging. Here, we compared age-related differences in the cortical differentiation of sensory vs. categorical features using a novel DNN-based representational similarity analysis approach (Güçlü and van Gerven, 2015; Khaligh-Razavi and Kriegeskorte, 2014; Kriegeskorte, 2015; Leeds et al., 2013; Wen et al., 2017).

Consistent with our hypothesis, within early visual cortex, we found evidence for age-related neural dedifferentiation of sensory features, where, compared to the YAs, brain activation patterns in early visual cortex exhibited a worse fit with the sensory model in the OAs (Fig. 2a); this finding was also replicated by using the more traditional HMAX model (Fig. 2b). It is well known that increased age is associated with a robust decline in visual performance (Monge and Madden, 2016; Owsley, 2011). Our finding suggests that this decline may not only be the result of a decline in perceptual operations (*processes*) performed on visual information but also a deficit in the quality of visual information itself (*representations*).

In contrast to sensory features in early visual cortex, we found that categorical features in the ATL were not just spared but actually enhanced within OAs. Within the ATL, compared to YAs, activation patterns had a better fit with the categorical model in the OAs (Fig. 2a); this finding was also replicated comparing within and between-category pattern similarity (Fig. 2c). Thus, in contrast to age-related dedifferentiation in early visual cortex, in the ATL, we found age-related hyperdifferentiation. As noted before, this is the first time this finding is reported. Regarding the regions that exhibited age-related hyperdifferentiation, the ATL is hypothesized to store prior knowledge (Lambon Ralph et al., 2017; Zhao et al., 2017) and, compared to YAs, OAs have a greater knowledge network (Long and Shaw, 2000; Park et al., 2002), likely from more years of knowledge accruement. It is likely that certain processes, such as conceptual and semantic processing, are more reliant on categorical features. Perhaps the enhanced categorical model-brain fit in the ATL within the OAs reflects OAs utilizing enhanced semantic knowledge in service of perception.

From this study it cannot be definitely determined exactly why this pattern of age-related dedifferentiation for sensory features and hyperdifferentiation for categorical features occurs, but we believe this may reflect age-related differences in strategies to complete this task. It may be the case that in order for YAs to successfully complete this task, it is more beneficial for them to encode the sensory features of the task stimuli, whereas in OAs, it is more beneficial for them to encode categorical features. Indeed, representations are not necessarily ‘hard-wired’ into the brain and the

representational space can be warped in response to task demands (Martin et al., 2018; Wang et al., 2018). In order to confirm our interpretation of the results, a study manipulating participants' use of sensory and categorical representations is necessary.

4.2. Age-related differences in mnemonic representations

Our second question examined age-related differences in mnemonic representations. To examine this question, we examined the *reactivation* of mnemonic representations, which was assessed as the similarity between activation patterns during encoding and retrieval (ERS). Consistent with previous studies (Johnson et al., 2015; St-Laurent et al., 2014), compared to the YAs, in the OAs ERS was weaker in the early visual cortex (Fig. 4a). Given that we also found age-related dedifferentiation of sensory representations in this region, the age-related attenuation of ERS in early visual cortex likely reflects a negative impact of degraded sensory features on visual memories. It should be noted that even though there are studies that have also demonstrated attenuated reactivation within the visual cortex (Johnson et al., 2015; St-Laurent et al., 2014), three previous studies did not find this pattern (Abdulrahman et al., 2017; Thakral et al., 2019; Wang et al., 2016). These studies used multi-voxel pattern analysis (MVPA) to identify the reactivation of *classes of stimuli* (e.g, words vs. objects), whereas we used ERS to detect the reactivation of individual items. Thus, it is possible that MVPA is less sensitive than ERS in detecting age-related reactivation deficits. We also found an age-related ERS reduction in the hippocampus (Fig. 4a). This finding is consistent with evidence of impaired hippocampal activity in OAs (Kennedy et al., 2017; Nyberg, 2017), and it extends this evidence to multivariate activation patterns. The use of ERS to investigate hippocampal memory representations could be useful not only for investigating normal aging but also hippocampal dysfunction in Alzheimer's disease.

Finally, we found that, compared to YAs, OAs exhibited enhanced ERS in the ATL (Fig. 4a). As the ATL has been associated with abstract semantic representations (Lambon Ralph et al., 2017; Zhao et al., 2017), enhanced ATL ERS in OAs may reflect a greater reliance on semantic knowledge in service

of memory. This idea is consistent with our finding of age-related hyperdifferentiation for categorical features in this region (Fig. 2a). Supporting the importance of ATL representational quality for memory in aging, we found that in OAs, increased item-specific ERS in the ATL was associated with better performance on the post-scan memory recognition task (Fig. 4c). This across-subject correlation suggests that individual differences in memory performance may be at least partially mediated by neural representational quality.

The link of enhanced ERS in the ATL to better memory performance in OAs suggests that these representational changes are compensatory. In functional neuroimaging of aging, the term compensation has been typically applied to age-related increases in univariate activity, which are normally assumed to reflect differences in processes. However, there is no reason why compensatory mechanisms must be mediated only by processes and could not involve an enhancement in representations. In fact, the accumulation of knowledge during the lifespan is likely to lead to more distinct and detailed semantic representations, which could partially counteract the degraded quality of sensory representations. This is any intriguing possibility and further research is required to link enhanced ERS in OAs to functional compensation.

4.3. Conclusions

The traditional idea that aging is associated with a generalized decline in cognitive abilities and their underlying neural mechanisms has been challenged by evidence that although some cognitive and brain mechanisms are impaired by aging, others are not only spared but even enhanced by aging (Long and Shaw, 2000; Park et al., 2002). One aspect of cognition that is spared by aging are processes that rely on categorical features, such as conceptual and semantic processing, but the neural mechanisms of these spared functions are largely unknown. The results of the present study suggest that one factor contributing to the preservation of these processes in old age is the enhanced quality of categorical representations in the ATL. These spared categorical representations may contribute not only to perceptual but also to mnemonic aspects of cognition. Lastly, these findings have

implications not only for understanding normal aging but also the effects of pathological aging (e.g., Alzheimer's disease), which, to our knowledge, has yet to be examined.

5. Acknowledgements

This work was supported by the National Institute on Aging (R01 AG019731 awarded to RC and F31 AG060691 awarded to ZAM) and National Institute of Mental Health (F31 MH114454 to BRG). The funding agency had no role in the decision to publish or in the preparation of the manuscript. The authors do not have any conflicts of interest to report.

6. References

Abdulrahman, H., Fletcher, P.C., Bullmore, E., Morcom, A.M., 2017. Dopamine and memory dedifferentiation in aging. Neuroimage 153, 211-220.

Ashburner, J., 2007. A fast diffeomorphic image registration algorithm. Neuroimage 38(1), 95-113.

Baltes, P.B., Lindenberger, U., 1997. Emergence of a powerful connection between sensory and cognitive functions across the adult life span: A new window to the study of cognitive aging? Psychol. Aging 12, 12-21.

Bankson, B.B., Hebart, M.N., Groen, I.I.A., Baker, C.I., 2018. The temporal evolution of conceptual object representations revealed through models of behavior, semantics and deep neural networks. Neuroimage 178, 172-182.

Bussey, T.J., Saksida, L.M., Murray, E.A., 2005. The perceptual-mnemonic/feature conjunction model of perirhinal cortex function. The Quarterly journal of experimental psychology. B, Comparative and physiological psychology 58(3-4), 269-282.

Cadieu, C.F., Hong, H., Yamins, D.L., Pinto, N., Ardila, D., Solomon, E.A., Majaj, N.J., DiCarlo, J.J., 2014. Deep neural networks rival the representation of primate IT cortex for core visual object recognition. PLoS Comput Biol 10(12), e1003963.

Carp, J., Park, J., Polk, T.A., Park, D.C., 2011. Age differences in neural distinctiveness revealed by multi-voxel pattern analysis. Neuroimage 56(2), 736-743.

Chee, M.W.L., Goh, J.O.S., Venkatraman, V., Tan, J.C., Gutchess, A., Sutton, B., Hebrank, A., Leshikar, E., Park, D., 2006. Age-related changes in object processing and contextual binding revealed using fMR adaptation. J Cogn Neurosci 18(4), 495-507.

Cherry, K.E., Silva Brown, J., Jackson Walker, E., Smitherman, E.A., Boudreaux, E.O., Volaufova, J., Michal Jazwinski, S., 2012. Semantic encoding enhances the pictorial superiority effect in the oldest-old. Neuropsychol Dev Cogn B Aging Neuropsychol Cogn 19(1-2), 319-337.

Clarke, A., Pell, P.J., Ranganath, C., Tyler, L.K., 2016. Learning warps object representations in the ventral temporal cortex. J Cogn Neurosci 28(7), 1010-1023.

Clarke, A., Tyler, L.K., 2014. Object-specific semantic coding in human perirhinal cortex. J Neurosci 34(14), 4766-4775.

Danker, J.F., Anderson, J.R., 2010. The Ghosts of Brain States Past: Remembering Reactivates the Brain Regions Engaged During Encoding. Psychol. Bull. 136(1), 87-102.

Devereux, B.J., Clarke, A.D., Tyler, L.K., 2018. Integrated deep visual and semantic attractor neural networks predict fMRI pattern-information along the ventral object processing pathway. Scientific reports 8(1), 10636.

Folstein, M.F., Folstein, S.E., McHugh, P.R., 1975. "Mini-mental state". A practical method for grading the cognitive state of patients for the clinician. J Psychiatr Res 12(3), 189-198.

Geib, B.R., Stanley, M.L., Wing, E.A., Laurienti, P.J., Cabeza, R., 2017. Hippocampal contributions to the large-scale episodic memory network predict vivid visual memories. Cereb Cortex 27(1), 680-693.

Gilmore, G.C., Spinks, R.A., Thomas, C.W., 2006. Age effects in coding tasks: Componential analysis and test of the sensory deficit hypothesis. Psychol. Aging 21(1), 7-18.

Goh, J.O., Suzuki, A., Park, D.C., 2010. Reduced neural selectivity increases fMRI adaptation with age during face discrimination. Neuroimage 51(1), 336-344.

Grady, C., 2012. The cognitive neuroscience of ageing. Nat Rev Neurosci 13(7), 491-505.

Grady, C.L., 2008. Cognitive neuroscience of aging. Annals of the New York Academy of Sciences 1125(1), 127-144.

Groen, II, Greene, M.R., Baldassano, C., Fei-Fei, L., Beck, D.M., Baker, C.I., 2018. Distinct contributions of functional and deep neural network features to representational similarity of scenes in human brain and behavior. eLife 7.

Güçlü, U., van Gerven, M.A.J., 2015. Deep neural networks reveal a gradient in the complexity of neural representations across the ventral stream. J Neurosci 35(27), 10005-10014.

Hodges, J.R., Patterson, K., Oxbury, S., Funnell, E., 1992. Semantic dementia. Progressive fluent aphasia with temporal lobe atrophy. Brain : a journal of neurology 115 (Pt 6), 1783-1806.

Johnson, M.K., Kuhl, B.A., Mitchell, K.J., Ankudowich, E., Durbin, K.A., 2015. Age-related differences in the neural basis of the subjective vividness of memories: evidence from multivoxel pattern classification. Cogn Affect Behav Neurosci 15(3), 644-661.

Kausler, D.H., 1994. Learning and memory in normal aging. Academic Press, San Diego, CA.

Kennedy, K.M., Boylan, M.A., Rieck, J.R., Foster, C.M., Rodrigue, K.M., 2017. Dynamic range in BOLD modulation: lifespan aging trajectories and association with performance. Neurobiol Aging 60, 153-163.

Khaligh-Razavi, S.M., Kriegeskorte, N., 2014. Deep supervised, but not unsupervised, models may explain IT cortical representation. PLoS Comput Biol 10(11), e1003915.

Koen, J.D., Rugg, M.D., 2016. Memory reactivation predicts resistance to retroactive interference: evidence from multivariate classification and pattern similarity analyses. J Neurosci 36(15), 4389-4399.

Kriegeskorte, N., 2015. Deep neural networks: a new framework for modeling biological vision and brain information processing. Annu Rev Vis Sci 1(1), 417-446.

Kriegeskorte, N., Douglas, P.K., 2018. Cognitive computational neuroscience. Nat Neurosci 21(9), 1148-1160.

Kriegeskorte, N., Goebel, R., Bandettini, P., 2006. Information-based functional brain mapping. Proc Natl Acad Sci U S A 103(10), 3863-3868.

Kriegeskorte, N., Kievit, R.A., 2013. Representational geometry: integrating cognition, computation, and the brain. Trends Cogn Sci 17(8), 401-412.

Kriegeskorte, N., Mur, M., Bandettini, P., 2008. Representational similarity analysis–connecting the branches of systems neuroscience. Front Syst Neurosci 2, 4.

Krizhevsky, A., Sutskever, I., Hinton, G.E., 2012. Imagenet classification with deep convolutional neural networks, Advances in Neural Information Processing Systems. pp. 1097-1105.

Lambon Ralph, M.A., Jefferies, E., Patterson, K., Rogers, T.T., 2017. The neural and computational bases of semantic cognition. Nat Rev Neurosci 18(1), 42-55.

LeCun, Y., Bengio, Y., Hinton, G., 2015. Deep learning. Nature 521(7553), 436-444.

Leeds, D.D., Seibert, D.A., Pyles, J.A., Tarr, M.J., 2013. Comparing visual representations across human fMRI and computational vision. J Vis 13(13), 25-25.

Lindenberger, U., Baltes, P.B., 1994. Sensory functioning and intelligence in old age: A strong connection. Psychol. Aging 9, 339-355.

Long, L.L., Shaw, R.J., 2000. Adult age differences in vocabulary acquisition. Educational Gerontology 26(7), 651-664.

Martin, C.B., Douglas, D., Newsome, R.N., Man, L.L., Barense, M.D., 2018. Integrative and distinctive coding of visual and conceptual object features in the ventral visual stream. eLife 7.

Mohanty, P., Naveh-Benjamin, M., Ratneshwar, S., 2016. Beneficial effects of semantic memory support on older adults' episodic memory: differential patterns of support of item and associative information. Psychol Aging 31(1), 25-36.

Monge, Z.A., Madden, D.J., 2016. Linking cognitive and visual perceptual decline in healthy aging: the information degradation hypothesis. Neurosci Biobehav Rev 69, 166-173.

Mumford, J.A., Turner, B.O., Ashby, F.G., Poldrack, R.A., 2012. Deconvolving BOLD activation in event-related designs for multivoxel pattern classification analyses. Neuroimage 59(3), 2636-2643.

Murphy, D.R., Craik, F.I., Li, K.Z., Schneider, B.A., 2000. Comparing the effects of aging and background noise on short-term memory performance. Psychol Aging 15(2), 323-334.

Naveh-Benjamin, M., 2000. Adult age differences in memory performance: Tests of an associative deficit hypothesis. Journal of Experimental Psychology: Learning, Memory, & Cognition 26(5), 1170-1187.

Nyberg, L., 2017. Functional brain imaging of episodic memory decline in ageing. Journal of internal medicine 281(1), 65-74.

Owsley, C., 2011. Aging and vision. Vision Res 51(13), 1610-1622.

Park, D.C., Lautenschlager, G., Hedden, T., Davidson, N.S., Smith, A.D., Smith, P.K., 2002. Models of visuospatial and verbal memory across the adult life span. Psychol Aging 17(2), 299-3320.

Park, D.C., Polk, T.A., Park, R., Minear, M., Savage, A., Smith, M.R., 2004. Aging reduces neural specialization in ventral visual cortex. Proc Natl Acad Sci U S A 101(35), 13091-13095.

Payer, D., Marshuetz, C., Sutton, B., Hebrank, A., Welsh, R.C., Park, D.C., 2006. Decreased neural specialization in old adults on a working memory task. Neuroreport 17(5), 487-491.

Pichora-Fuller, M.K., Schneider, B.A., Daneman, M., 1995. How young and old adults listen to and remember speech in noise. J Acoust Soc Am 97(1), 593-608.

Riesenhuber, M., Poggio, T., 1999. Hierarchical models of object recognition in cortex. Nat Neurosci 2(11), 1019-1025.

Ritchey, M., Wing, E.A., LaBar, K.S., Cabeza, R., 2013. Neural similarity between encoding and retrieval is related to memory via hippocampal interactions. Cereb Cortex 23(12), 2818-2828.

Rugg, M.D., Vilberg, K.L., 2013. Brain networks underlying episodic memory retrieval. Curr. Opin. Neurobiol. 23(2), 255-260.

Sarkka, S., Solin, A., Nummenmaa, A., Vehtari, A., Auranen, T., Vanni, S., Lin, F.H., 2012. Dynamic retrospective filtering of physiological noise in BOLD fMRI: DRIFTER. Neuroimage 60(2), 1517-1527.

Seabold, S., Perktold, J., 2010. Statsmodels: econometric and statistical modeling with Python, Proceedings of the 9th Python in Science Conference. p. 61.

Serre, T., Wolf, L., Bileschi, S., Riesenhuber, M., Poggio, T., 2007. Robust object recognition with cortex-like mechanisms, IEEE Trans Pattern Anal Mach Intell, 2007/01/17 ed., pp. 411-426.

Simonyan, K., Zisserman, A., 2014. Very deep convolutional networks for large-scale image recognition. arXiv, 1409.1556.

St-Laurent, M., Abdi, H., Bondad, A., Buchsbaum, B.R., 2014. Memory reactivation in healthy aging: evidence of stimulus-specific dedifferentiation. J Neurosci 34(12), 4175-4186.

Thakral, P.P., Wang, T.H., Rugg, M.D., 2019. Effects of age on across-participant variability of cortical reinstatement effects. Neuroimage 191, 162-175.

Tyler, L.K., Stamatakis, E.A., Bright, P., Acres, K., Abdallah, S., Rodd, J.M., Moss, H.E., 2004. Processing objects at different levels of specificity. J Cogn Neurosci 16(3), 351-362.

Tzourio-Mazoyer, N., Landeau, B., Papathanassiou, D., Crivello, F., Etard, O., Delcroix, N., Mazoyer, B., Joliot, M., 2002. Automated anatomical labeling of activations in SPM using a macroscopic anatomical parcellation of the MNI MRI single-subject brain. Neuroimage 15(1), 273-289.

Voss, M.W., Erickson, K.I., Chaddock, L., Prakash, R.S., Colcombe, S.J., Morris, K.S., Doerksen, S., Hu, L., McAuley, E., Kramer, A.F., 2008. Dedifferentiation in the visual cortex: an fMRI investigation of individual differences in older adults. Brain Res 1244, 121-131.

Wang, T.H., Johnson, J.D., de Chastelaine, M., Donley, B.E., Rugg, M.D., 2016. The effects of age on the neural correlates of recollection success, recollection-related cortical reinstatement, and post-retrieval monitoring. Cereb Cortex 26(4), 1698-1714.

Wang, W.C., Brashier, N.M., Wing, E.A., Marsh, E.J., Cabeza, R., 2018. Neural basis of goal-driven changes in knowledge activation. The European journal of neuroscience 48(11), 3389-3396.

Warrington, E.K., McCarthy, R., 1983. Category specific access dysphasia. Brain : a journal of neurology 106 (Pt 4), 859-878.

Wen, H., Shi, J., Zhang, Y., Lu, K.H., Cao, J., Liu, Z., 2017. Neural encoding and decoding with deep Learning for dynamic natural vision. Cereb Cortex, 1-25.

Wing, E.A., Ritchey, M., Cabeza, R., 2014. Reinstatement of individual past events revealed by the similarity of distributed activation patterns during encoding and retrieval. J Cogn Neurosci 27(4), 679-691.

Zeiler, M.D., Fergus, R., 2014. Visualizing and understanding convolutional networks, European Conference on Computer Vision. Springer International Publishing, Cham, pp. 818-833.

Zhao, Y., Song, L., Ding, J., Lin, N., Wang, Q., Du, X., Sun, R., Han, Z., 2017. Left anterior temporal lobe and bilateral anterior cingulate cortex are semantic hub regions: Evidence from behavior-nodal degree mapping in brain-damaged patients. Journal of Neuroscience 37(1), 141-151.

Zhou, B., Lapedriza, A., Khosla, A., Oliva, A., Torralba, A., 2017. Places: A 10 million image database for scene recognition. IEEE Transactions on Pattern Analysis and Machine Intelligence(99).

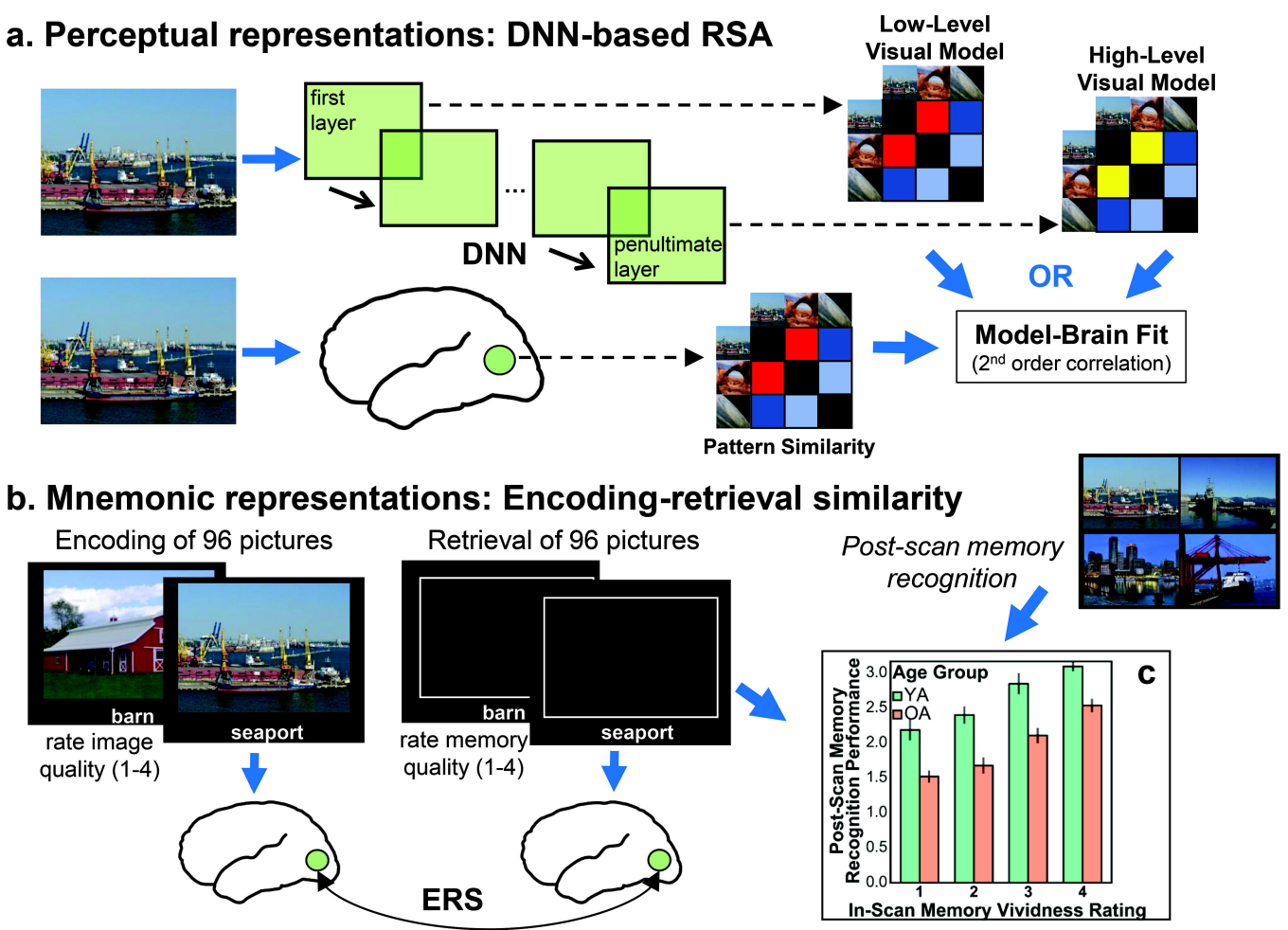
a. Perceptual representations: DNN-based RSA
Low-Level Visual Model
High-Level Visual Model
first layer
DNN
penultimate layer
OR
Model-Brain Fit
(2nd order correlation)
Pattern Similarity
b. Mnemonic representations: Encoding-retrieval similarity
Encoding of 96 pictures
Retrieval of 96 pictures
Post-scan memory recognition
barn
seaport
rate image quality (1-4)
rate memory quality (1-4)
ERS
Age Group
YA
OA
Post-Scan Memory Recognition Performance
In-Scan Memory Vividness Rating
C

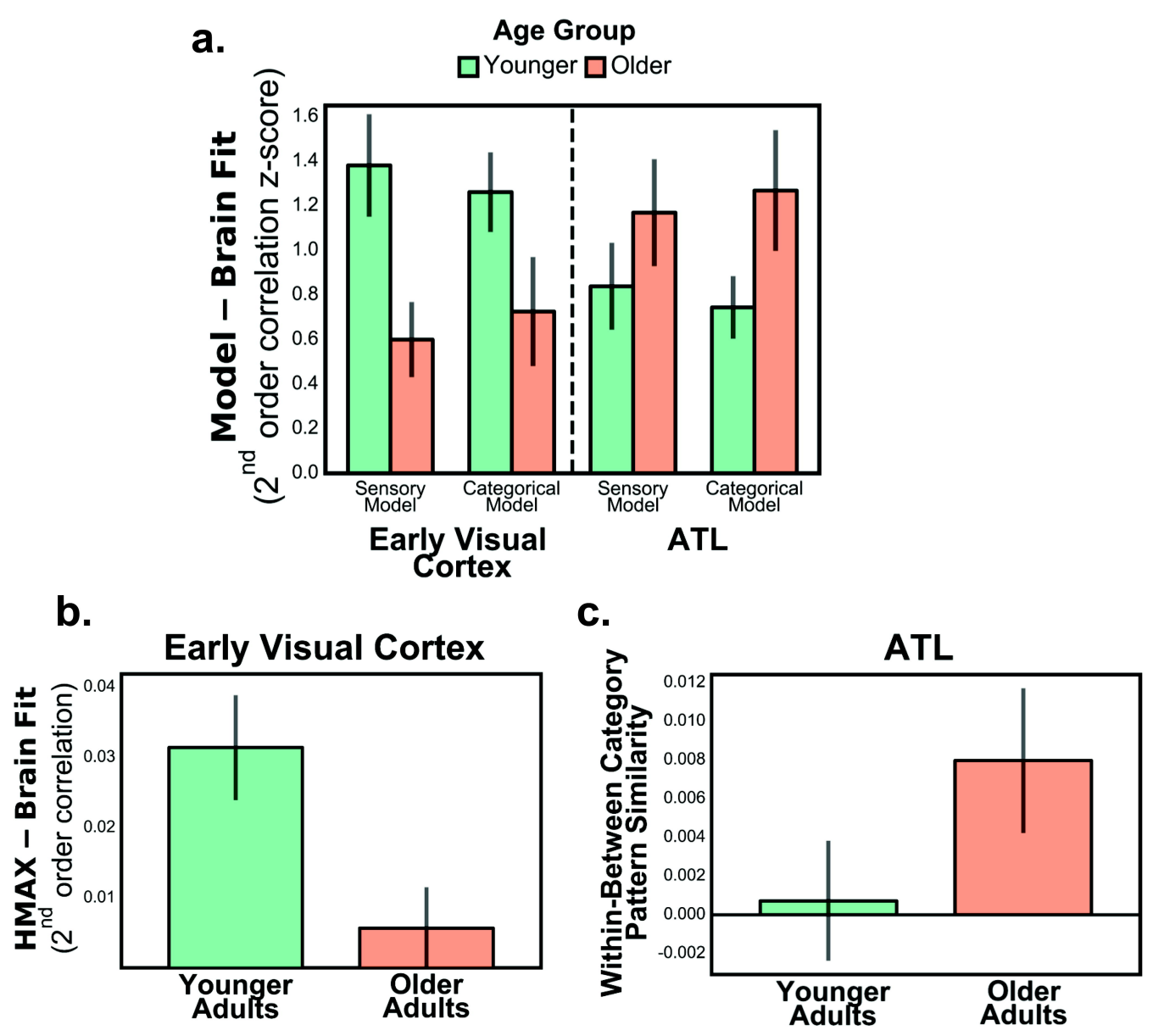
a.
Age Group
Younger
Older
Model – Brain Fit
(2nd order correlation z-score)
1.6
1.4
1.2
1.0
0.8
0.6
0.4
0.2
0.0
Sensory Model
Categorical Model
Sensory Model
Categorical Model
Early Visual Cortex
ATL
b.
Early Visual Cortex
HMAX – Brain Fit
(2nd order correlation)
0.04
0.03
0.02
0.01
Younger Adults
Older Adults
c.
ATL
Within-Between Category Pattern Similarity
0.012
0.010
0.008
0.006
0.004
0.002
0.000
-0.002
Younger Adults
Older Adults

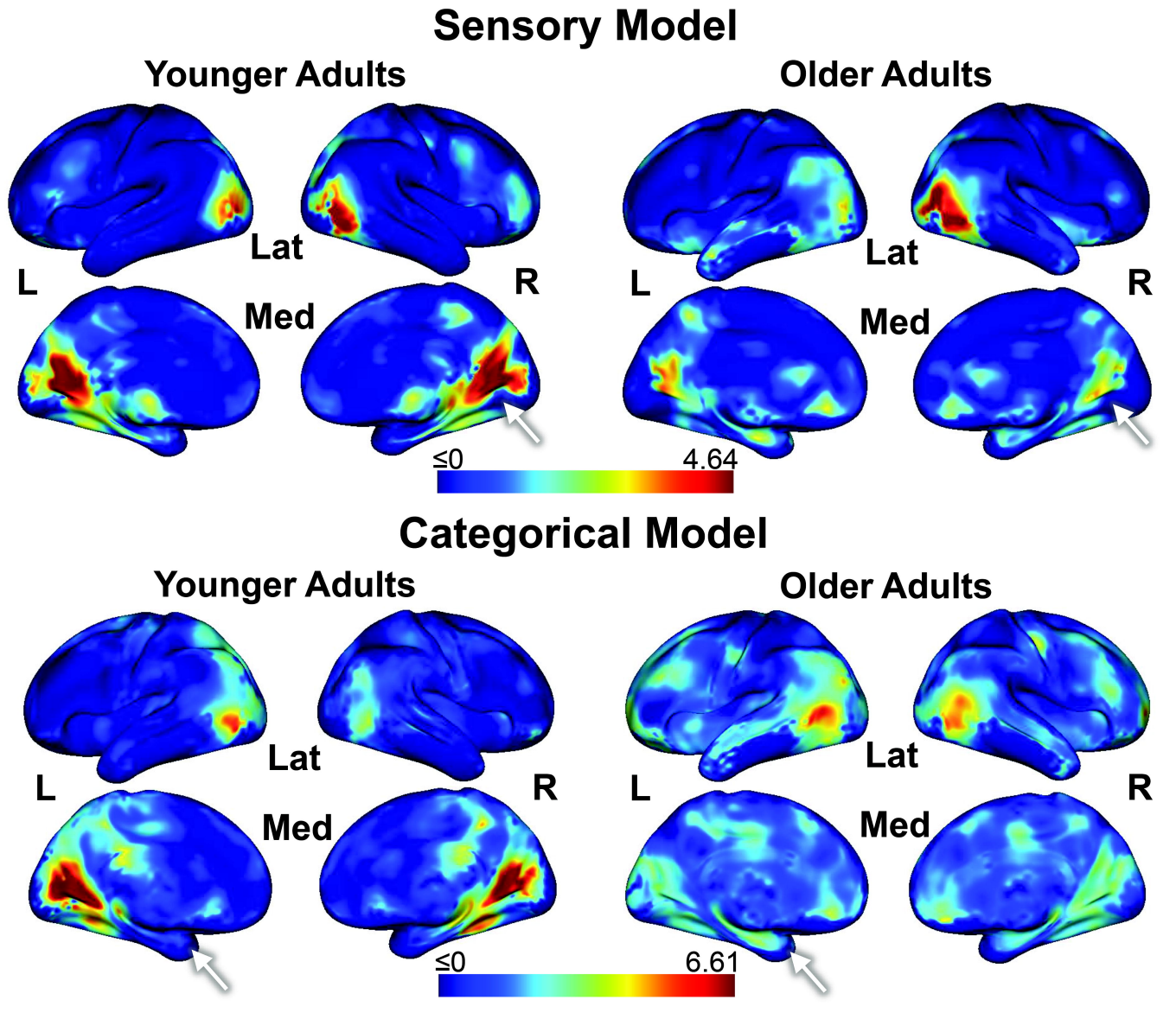
Sensory Model
Younger Adults
Older Adults
Lat
Med
L
R
≤0
4.64
Categorical Model
Younger Adults
Older Adults
Lat
Med
L
R
≤0
6.61

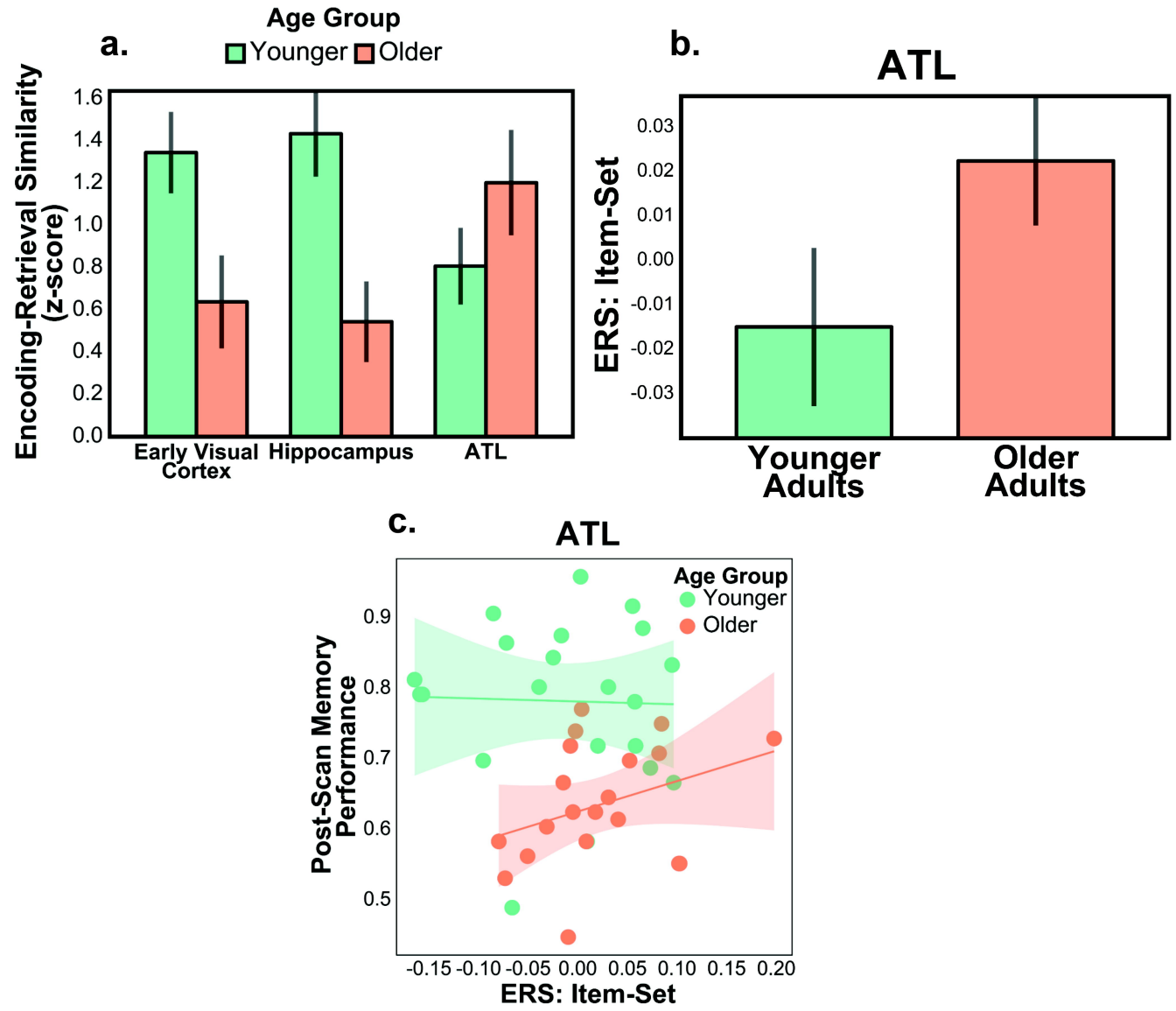
a.
Age Group
Younger
Older
Encoding-Retrieval Similarity (z-score)
1.6
1.4
1.2
1.0
0.8
0.6
0.4
0.2
0.0
Early Visual Cortex
Hippocampus
ATL
b.
ATL
ERS: Item-Set
0.03
0.02
0.01
0.00
-0.01
-0.02
-0.03
Younger Adults
Older Adults
c.
ATL
Age Group
Younger
Older
Post-Scan Memory Performance
0.9
0.8
0.7
0.6
0.5
-0.15 -0.10 -0.05 0.00 0.05 0.10 0.15 0.20
ERS: Item-Set